nucleate boiling heat flux and the wettability exhibited a maximum and minimum respectively at approximately 1.9 mpl %. For the surfactant systems there was no detectable change in intensity with concentration for the sodium lauryl sulphate mixtures, and a very small reduction in intensity with concentration when using lauryl alcohol. Thus we deduce that the sound emissions are only dependent on the quality of the vapour inside the bubble, that is for the alcohol system a steady increase in concentration results in a steady decrease in sound intensity. For the sodium lauryl suphate solution, although the surface tension of the system falls significantly with an increase of concentration the vapour will be that of water and no change in intensity is noted. The lauryl alcohol has a small but higher vapour pressure and a slight reduction in intensity occurs.

Since there is no peak in the intensity–concentration curve for ethanol it is evident that the sounds are emitted when the bubbles collapse away from the wire surface. It also demonstrates that the heat transfer is controlled by the bubble formation on the metal surface and not influenced by the bubble implosion away from the wire.

REFERENCES

1. S. J. D. van Stralen, M. S. Sohal, R. Cole and W. M. Sluyter, Bubble growth rates in pure and binary systems; combined effect of relaxation and evaporation microlayers, *Int. J. Heat Mass Transfer* **18**, 453 (1975).
2. A. S. Vos and S. J. D. van Stralen, Heat transfer to boiling water–methylethylketone mixtures, *Chem. Engng. Sci.* **5**, 50 (1956).
3. N. Isshiki and I. Nikai, Boiling of binary mixtures, *Heat Transfer (Japan. Res.)* **1**, 56 (1972).
4. J. Hovestreijdt, The influence of the surface tension difference on the boiling of mixtures, *Chem. Engng. Sci.* **18**, 631 (1963).
5. A. B. Ponter, E. L. Maddox, P. Trauffler and S. Vijayan, Maximale Wärmeflussdichte in Zweistoffsystemen, *Verfahrenstechnik* **10**, 443 (1976).
6. A. B. Ponter and C. P. Haigh, Sound emission and heat transfer in low pressure pool boiling, *Int. J. Heat Mass Transfer* **12**, 413 (1969).
7. C. P. Haigh and A. B. Ponter, Sound emission from boiling on a submerged wire, *Can. J. Chem. Engng.* **49**, 309 (1971).

Int. J. Heat Mass Transfer. Vol. 20, pp. 1262–1265. Pergamon Press 1977. Printed in Great Britain

INFRARED RADIATION PROPERTIES OF NITROUS OXIDE IN THE 4.5μ REGION

M. NIKANJAM and R. GREIF
Department of Mechanical Engineering, University of California, Berkeley, CA 94720, U.S.A.

(*Received* 22 *September* 1976 *and in revised form* 15 *November* 1976)

NOMENCLATURE

T, temperature;
T_r, room temperature;
X, pressure path length.

Greek symbols

ε, emissivity;
λ, wavelength;
τ, transmission coefficient.

Subscripts

c, calibration source;
r, room condition.

INTRODUCTION

IN THIS study the IR emission of the 4.5μ combination band of nitrous oxide has been measured at temperatures of 1200, 1700 and 1900°K. The high temperature gas was produced in a shock tube and measurements were carried out in the end wall region behind the reflected shock wave for the high temperature cases, 1700 and 1900°K. The region behind the incident shock wave was utilized for the 1200°K case.

Previous spectral measurements of the 4.5μ band of nitrous oxide have been made by Burch and Williams [1] at room temperature and by Tien, Modest and McCreight [2] at room temperature and at 500°K. There do not appear to be any data available at higher temperatures.

EXPERIMENTAL APPARATUS

The experiments were carried out in a free piston shock tube which uses a piston compression in the driver section to obtain the desired driver conditions of pressure, P_4, and temperature, T_4, behind the diaphragm (cf. Fig. 1). The diaphragm, which separates the driver gas* from the test or driven gas, ruptures due to the pressure difference, $P_4 - P_1$, and a shock wave forms which propagates in the test section. The speed of the shock wave was determined from the outputs from thin film platinum thermometers. A description of the system which includes details of the piston release mechanism and other considerations is presented in [3]. References [4–8] may also be referred to for discussions of free piston shock tubes.

The aluminum test or expansion section is 2.7 m long with a 7.6 cm square cross section and a 3 mm wall thickness. For the measurements that were made behind the reflected shock wave, corresponding to region 5, the optical window was located 3.8 cm in front of the end wall. This was the condition for the 1700 and 1900°K cases. For the 1200°K case, emission measurements were made in region 2 behind the incident shock wave. This was accomplished by using an extension so that the optical window was then located 27.9 cm from the end wall. This long distance between the window and the end wall provided sufficient time for radiation measurements to be made in region 2 before the arrival of the reflected shock wave.

The radiation emitted from the shock heated gas was first passed through a Kodak Irtran 3 window (manufactured by the Eastman Kodak Co.) which had a useful transmission range from 0.4 to 11.5μ. The rays were then directed and focussed by a combination of plane and spherical mirrors upon the entrance slits of a 0.5 m McPherson grating poly-

*The driver region behind the diaphragm contained only nitrogen for the 1700 and 1900°K cases, while a mixture of nitrogen and helium was used for the 1200°K case.

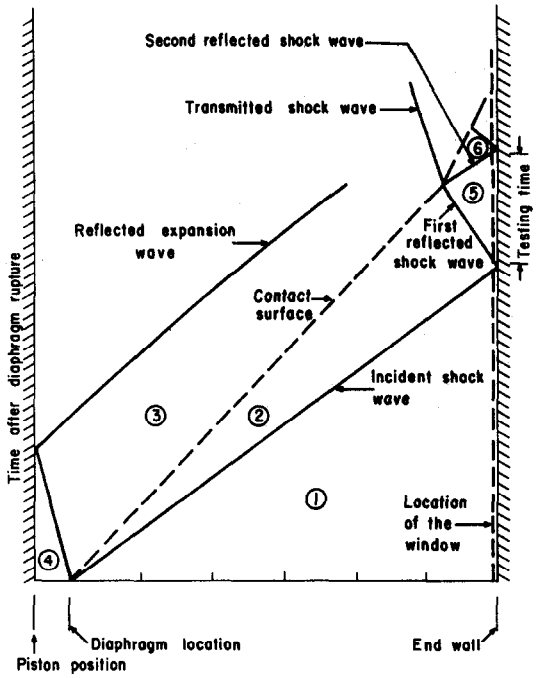

FIG. 1. Flow regimes in the shock tube.

chromator. A long wavelength pass filter was placed at the entrance slits to prevent extraneous radiation from the shorter wavelengths, $\lambda/2$, $\lambda/3$, etc., from entering the spectrometer. The filter has a cut off at 3.08 μ. A collimating mirror directed the radiation upon the 160 lines/mm grating. The radiation was then reflected onto a focussing mirror which directed the rays onto two exit slits which were 1 mm wide and 16.5 mm apart. The resolution for the system at a wavelength of 4.5 μ was 6.8 cm^{-1} (0.014 μ). An indium antimonide photovoltaic infrared detector (Philco ISC-363) was used to detect the radiation. The detector, which operated at liquid nitrogen temperature, approximately 77°K, had a cut off wavelength near 5 μ and a detectivity D^* of 6×10^9 cm $Hz^{1/2}/W$. The optical pathlength was 7.0 cm. A Tektronix 565A oscilloscope was used to record the signal from the detector. An absolute intensity calibration was made with both a standard globar and an IR Industries 463 blackbody source. The calibration was carried out over the entire range of wavelengths studied and, in particular, at every wavelength at which experimental data were recorded.

RESULTS AND DISCUSSION

The radiation emitted by nitrous oxide in the 4.5 μ region is discussed in [9]. Typical oscillograms for the emission measurements are shown in Figs. 2 and 3. As shown in Fig. 2, the voltage output from the photovoltaic infrared detector increases after the gas is heated by the incident shock wave. The vertical scale is 0.02 V/div. The speed of the shock wave is determined from the output of the thin film resistance thermometers which respond rapidly to the passage of the shock wave. Figure 3 is a typical oscillogram for the emission measurement for the gas in the end wall region behind the first reflected shock wave, denoted by region 5 in Fig. 1. The vertical scale is 0.05 V/div. For this measurement the optical window is located close to the end wall so that the effect of the incident shock wave cannot be distinguished from the contribution resulting from the passage of the reflected shock wave. For completeness, it is noted that the testing time in region 2 is limited by the arrival of the contact surface (cf. Figs. 1 and 2), while the testing time in region 5 is limited by the arrival of the second reflected shock wave (cf. Figs. 1 and 3).

The conditions behind the incident and the reflected shock waves are determined from the solution of the conservation equations of mass, momentum and energy. The results are based on the initial state of the gas and the speed (Mach number) of the shock wave. The initial pressure in the test section was 20 mm of Hg for all runs. For the measurements behind the incident shock wave, $T_2 = 1200°K$,

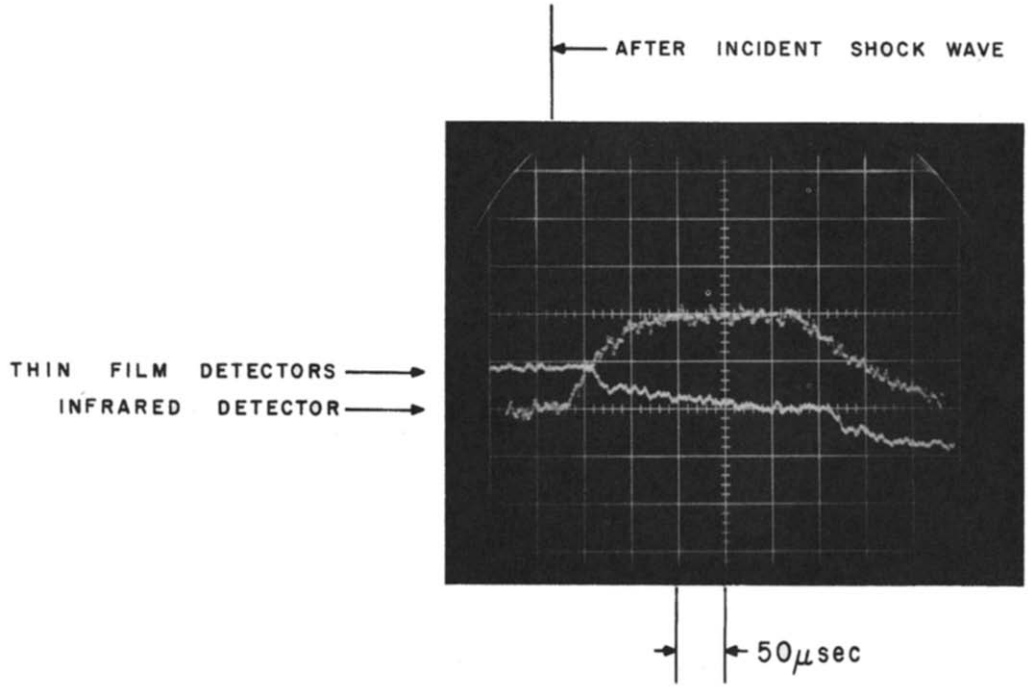

FIG. 2. Typical oscillogram for measurement behind incident shock wave. 35% N_2O, 65% He, $T_2 = 1200°K$, $P_2 = 0.53$ atm.

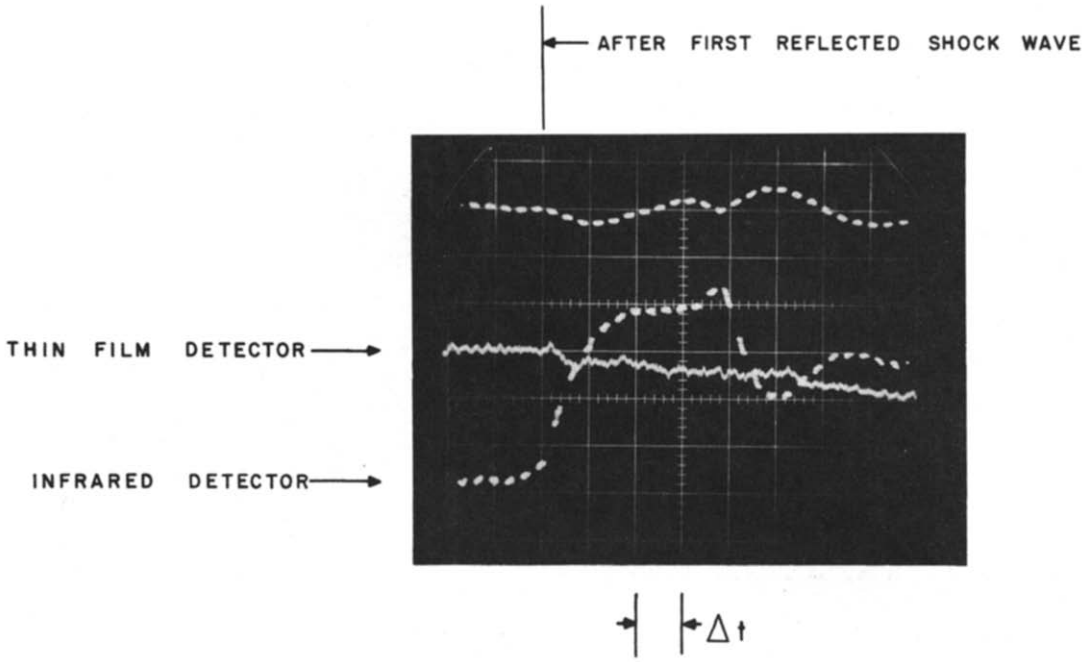

FIG. 3. Typical oscillogram for measurement behind reflected shock wave. 25% N_2O, 75% He, $T_5 = 1900°K$, $P_5 = 2.1$ atm. $\Delta t = 50\,\mu s$ for thin film detector, $100\,\mu s$ for IR detector.

$P_2 = 0.53$ atm, and the gas composition was 35% nitrous oxide and 65% helium. For the measurements behind the reflected shock wave the conditions were $T_5 = 1700°K$, $P_5 = 1.54$ atm, with 20% N_2O and 80% He, and $T_5 = 1900°K$, $P_5 = 2.10$ atm, with 25% N_2O and 75% He.

The determination of the radiative properties from the above results is obtained as follows. The voltage output from a narrow spectral region $\Delta\lambda$ due to radiative emission

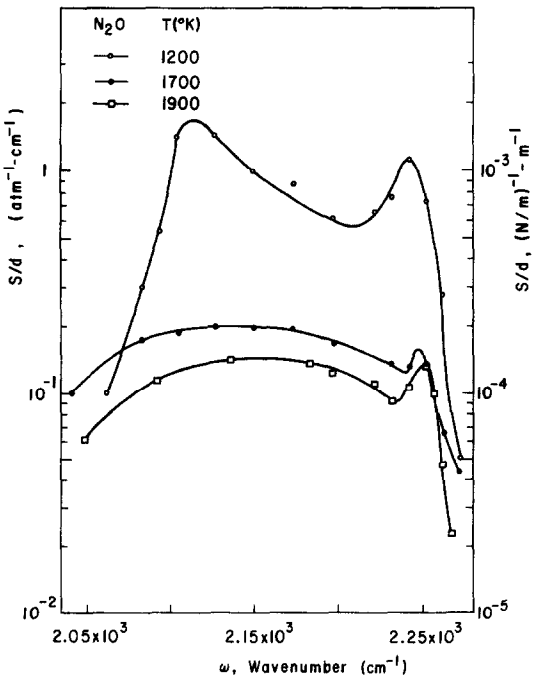

FIG. 4. Results for mean line intensity to spacing ratio.

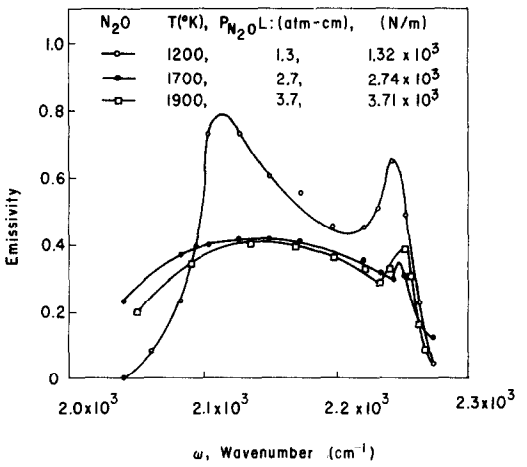

FIG. 5. Results for spectral emissivity. Runs *a*, *b*, *c*: $T(°K) = 1200$, 1700, 1900; $P_{total}(atm) = 0.53$, 1.54, 2.10; $P_{N_2O}(atm) = 0.19$, 0.31, 0.53.

from the shock heated gas at a temperature T is given by [3]:

$$V_{\lambda,T} = E_{b\lambda,T}\tau_{s\lambda}\left\{\int_{\Delta\lambda}\exp(-k_{\lambda,T_r}X)_{air}\,d\lambda - \int_{\Delta\lambda}\exp[(-k_{\lambda,T_r}X)_{air} - (k_{\lambda,T}X)_{N_2O}]\,d\lambda\right\} \quad (1)$$

where the blackbody radiance, $E_{b\lambda,T}$, and the spectral transmission coefficient, $\tau_{s\lambda}$, are evaluated at a given wavelength within the wavelength interval. The other quantities are defined in the Nomenclature. Now, if the shock tube is replaced by a calibration source having an emissivity ε_c at temperature T_c the voltage output is then given by

$$V_{\lambda,T_c} = \varepsilon_c E_{b\lambda,T_c}\tau_{s\lambda}\int_{\Delta\lambda}\exp(-k_{\lambda,T_r}X)_{air}\,d\lambda. \quad (2)$$

For well overlapped lines we introduce a mean line intensity,

$\bar{S}$, and a mean line spacing, d, over a narrow spectral interval according to (10)

$$\int_{\Delta\lambda} \exp(-k_\lambda X)\,d\lambda = \exp(-\bar{k}_\lambda X)\Delta\lambda = \exp(-\bar{S}X/d)\Delta\lambda. \quad (3)$$

Making this substitution in equations (1) and (2) yields the spectral emissivity (3):

$$\varepsilon_\lambda = 1 - \exp(-\bar{S}X/d)_{N_2O,T} = \frac{\varepsilon_c E_{b\lambda,T_c} V_{\lambda,T}}{E_{b\lambda,T} V_{\lambda,T_c}}. \quad (4)$$

Results for values of $\bar{S}/d$ and ε_λ may then be obtained and these are presented in Figs. 4 and 5, respectively. The limitations on the wavelength range are due primarily to the characteristics of the detector.

A band emissivity, ε, may also be obtained by integrating the spectral emissivity, ε_λ, according to $\int \varepsilon_\lambda E_{b\lambda}\,d\lambda / \int E_{b\lambda}\,d\lambda$, over the band width. For the 1200°K case with $P_{N_2O}L = 1.3$ atm cm, and $P_{total} = 0.53$ atm, a value of $\varepsilon = 0.027$ was obtained. For the higher temperature and higher pathlength cases the spectral data do not cover the entire band so that a band emissivity cannot be obtained from the data. However, carrying out the indicated integration over the range for which data is available, that is, from approximately 2050–2270 cm^{-1} yields values for the "partial" band emissivity of 0.013 for 1700°K, $P_{N_2O}L = 2.7$ atm cm, $P_{total} = 1.54$ atm, and 0.010 for 1900°K, $P_{N_2O}L = 3.66$ atm cm, $P_{total} = 2.10$ atm.

Acknowledgement—The authors acknowledge with appreciation the support of this research by the National Science Foundation.

REFERENCES

1. D. E. Burch and D. Williams, Total absorptance by nitrous oxide bands in the infrared, *Appl. Optics* **1**, 473–482 (1962).
2. C. L. Tien, M. F. Modest and C. R. McCreight, Infrared radiation properties of nitrous oxide, *J. Quant. Spectrosc. Radiative Transfer* **12**, 267–277 (1972).
3. T. C. Hsieh, A. Hashemi and R. Greif, Shock tube measurements of the emission of carbon dioxide in the 2.7 micron region, *J. Heat Transfer* **97**, 397–399 (1975).
4. R. J. Stalker, An investigation of free piston compression of shock tube drive gas, National Research Council of Canada, MT-44, Ottawa (1961).
5. R. J. Stalker and H. G. Horning, Two developments with free piston drivers, Proceedings of the Seventh International Shock Tube Symposium, Toronto, p. 241 (1969).
6. R. Greif and A. E. Bryson, Jr., Measurements in a free piston shock tube, *AIAA Jl* **3**, 183 (1965).
7. D. J. Collins, R. Greif and A. E. Bryson, Jr., Measurements of the thermal conductivity of helium in the temperature range 1600–6700 K, *Int. J. Heat Mass Transfer* **8**, 1209 (1965).
8. D. J. Collins, Measurement of the thermal conductivity of noble gases in the temperature range 1500–5000 K, *J. Heat Transfer* **88**, 52 (1966).
9. U. P. Oppenheim and U. Ben-Aryeh, A general method for the use of band models, with applications to infrared atmospheric absorption, *J. Quant. Spectrosc. Radiative Transfer* **4**, 559–570 (1964).
10. G. N. Plass, Models of spectral band absorption, *J. Opt. Soc. Am.* **48**, 690 (1958).